محاكاة التدفّق وتحليل الأداء لحفارة توربينية

*خالد سحنون، *عبد الرحمن بن بريك، **أحمد سعيد منصور و*أسامة رقيق

*مخبر نجاعة المعدات البترولية والمواد، جامعة محمد بوقرة، بومرداس، الجزائر

**قسم هندسة القوى الميكانيكية، كلية الهندسة، جامعة عين شمس، القاهرة، مصر

الخلاصة

الحفارات التوربينية هي توربينات هيدروليكية محورية تُستخدم في التنقيب عن المحروقات في الظروف القاسية. وتمتلك مزايا أكثر من تقنيات الحفر الأخرى لسماحها بسرعات دوران عالية، وعزم تدوير مرتفع. في هذا العمل، تم إجراء محاكاة عددية لتدفق طين حفر بنموذج نيوتوني من خلال مرحلة واحدة من هذا التوربين الذي يحتوى على الأرياش الثابتة والأرياش الدوارة. تم استخدام نموذج مستوى الخلط المستقر في عمليات المحاكاة لأخذ دوران الجزء الدوّار بعين الاعتبار إلى جانب تدفقات الخاصية المتوسطة المكانية. تم استخدام نموذج K-٤ لأخذ خصائص السريان المضطرب بعين الاعتبار. تم حساب معلّمات الأداء الرئيسية كدالة فى سرعة الدوران وتم التحقق من صحتها عن طريق المقارنة بالقياسات المعملية التى أُجريت على النموذج المعملى – الذى له نفس الأبعاد الهندسية المُستخدمة لنموذج المحاكاه – في ظروف التشغيل الحقيقية. وقد تم التوصل إلى اتفاق جيد بين قيم القدرة وبيانات عزم الدوران المُقدمة من طرف الشركة المُصَنِعة، ونتائج المحاكاة الخاصة بنا لنفس المتغيرات. تم عرض مجالات تدفق مختلفة مثل السرعة والضغط، والتي كان لها تأثير كبير على أداء التوربينات المدروسة. سيؤدي ذلك إلى اختيار أفضل لمتغيرات أداء آلة الحفر في ظروف العمل الحقيقية.

Flow simulation and performance analysis of a drilling turbine

Khaled Sahnoune*, Abderrahmane Benbrik*, Ahmed S. Mansour** and Rekik Oussama*

Laboratory of Petroleum Equipment Reliability and Materials, Université M'Hamed Bougara, Boumerdes, Algeria
**Mechanical Power Department, College of Engineering, Ain Shams University, Cairo, Egypt*
Corresponding Author: k.Sahnoune@univ-boumerdes.dz

ABSTRACT

Turbodrills are axial hydraulic turbines that are used in drilling hydrocarbons in extreme conditions, possessing advantages over other drilling techniques with their high speed of rotation, and higher operating torques.

In the present work, a numerical simulation of a Newtonian Drilling Mud flow was carried out through one stage of this turbine. The steady state mixing plane model was used for the simulations to take the rotation of the rotor into account besides the spatially averaged property fluxes of the flow. The turbulence k-ε model was used to consider the turbulence effects.

Key performance parameters are calculated in terms of rotation speed, and they are validated against the experimental data of the same model geometry in real operating conditions. A good agreement has been found between our simulation results and manufacturing parameters (power and torque data) for the same variables.

Various flow fields are presented such as velocity and pressure, which had a great influence on the performance of the studied turbine. This will lead to choose the best parameters configuration of an optimal field operation.

Keywords: Turbodrill; CFD; turbulence; drilling mud; CFX; performance analysis.

INTRODUCTION

The introduction should introduce the reader to the subject of the paper; a review of the previous works related to the topic of the paper has been performed. Turbodrills or downhole turbines have been used in petroleum industry over nearly one century ago. The first model was invented by the Russian engineer Kapelyushnikov in 1924. The need for such equipment has been motivated by the depletion of the majority of shallower hydrocarbons reservoirs and necessity to explore viable reservoir at greater depth. Therefore, deep drilling brings great challenges such as hard rock formations, high pressure, and high temperatures. In these conditions only, turbodrills have been proven to be successful, thanks to their all metallic construction, flexibility of mud fluids types, and compatibility with various models of drill bits (Neyrfor, 2004).
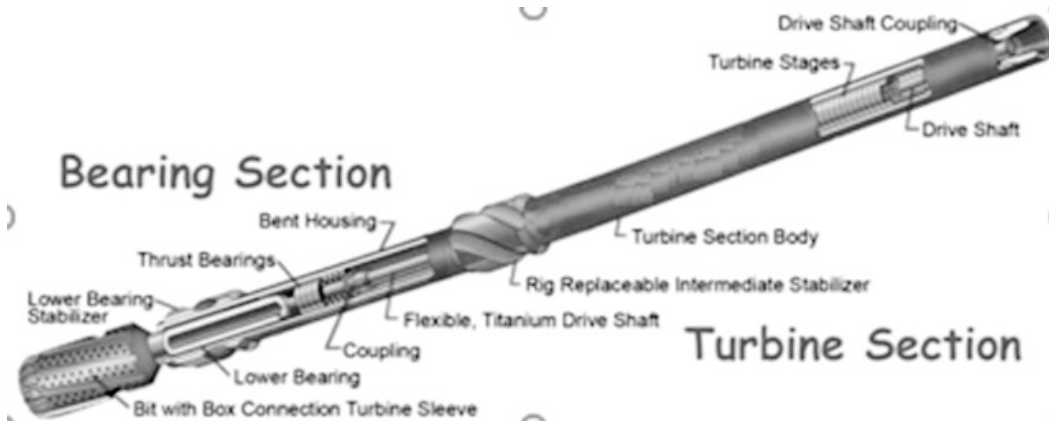
Fig. 1. Turbodrillschematic (Robert Radtke, 2011).

Turbodrills are hydraulic axial multistage turbines. Each stage consists of a stator and a rotor. All stages are identical, and the flow is purely axial as shown in Fig. 1. This machine converts the hydraulic power of high pressure mud fluid pumped from surface piston pumps into mechanical power by the interaction with rotor blades (Fig. 2). This power is then transmitted to the drill bit. In practice, multiple stages are stacked continuously until the required power and torque are achieved.
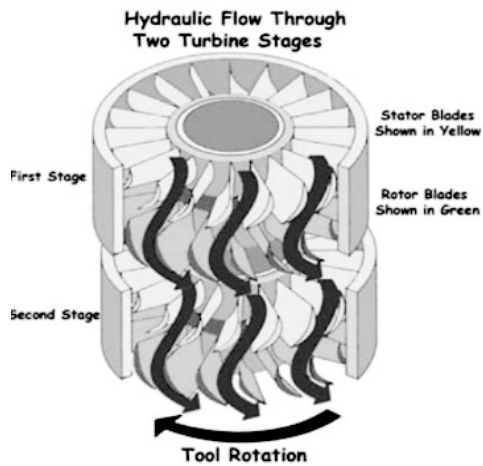

Fig. 2. Schematic of the flow through a drilling turbine stage (Neyrfor, 2004).

Using CFD simulations in order to study the flow fields and performance parameters of turbodrills has been a subject of interest of many recent researches. Mokaramian et al. (A. Mokaramian, 2012) (A. Mokaramian, 2015) presented a methodology for designing multistage turbodrill with asymmetric stator and rotor configuration.. The numerical simulations were carried out with different fluid types and various rotation speeds. It was found that the turbodrill performance is highly dependent on the rotation speed and mass flow rate values. This helped in finding the optimal operating values.

Mokaramian et al. (Mokaramian, Rasouli, & Cavanough, 2013) carried out a study on a small diameter turbodrill that was used for coiled tubing drilling in hard rock environment. A CFD analysis was used to analyze the fluid flow and performance (power and torque). In addition, a fluid structure study was carried out to measure the stress and deformation caused by fluid flow around turbine blades.

Zhang (Zhang, Yu, Gong, & Li, 2016) made an optimization study of a realistic turbine blade set tested using an experimental bench. Some improvements of blade geometry parameters were made by using the Box-Behenken response surface methodology. The new optimized design was used in a numerical CFD simulation to obtain new performance parameters, which were found to be very promising because there was an increase in the turbine efficiency by more than 10%.

Wang Yu (Wang Yu, 2014) used a blade profile optimization. Based on dimensionless coefficients, the new blade geometry was used in a CFD analysis. Based on the new blade geometry, full turbine stages were cast, and the prototype was experimentally tested on the experimental bench.

Montero et al. (V. G. Monteiro, 2017) made a performance evaluation of a turbodrill that was used in postsalt environment. Computational fluid dynamics was used for the numerical investigation. Two different drilling fluids were used, sea water and brine. Furthermore, multiple flow rates were tested to investigate how flow fields and performance are affected. The goal of their study was to find the best operational conditions for drilling in the working environment.

Wang et al. (Liguang Wang 2015) carried out a flow field analysis of a specific turbodrill model Φ127. The velocity and pressure distributions around turbine blades were simulated. The numerical work helped in performance predictions and finding the best suitable performance configuration to satisfy drilling tools requirements.

From previous reviewed literature, it is concluded that the new approach of designing and analyzing turbomachinery is based on CFD numerical studies. The same procedure was applied on a specific Turbodrill Model T122 Mk2 (Neyrfor Turbodrill Handbook, 2012), (Robert Radtke, 2011) for the current study. The flow field and performance curves will be studied. The numerical results will be validated against the performance curves provided by the manufacturer (Neyrfor Turbodrill Handbook, 2012). From the current studied literature, it was found that the comparisons between experimental work and the numerical one are not provided in most of the cases. On the other hand, in the few cases where the comparisons between the numerical and experimental work were provided, the numerical results were not in good agreement with experimental ones (Robert Radtke, 2011).

The mud that flows inside the turbodrill is water based; it is considered as a Newtonian fluid. This assumption was used by the turbine manufacturer for his testing (Neyrfor Turbodrill Handbook, 2012). The reason for this choice is related to the flow behavior, which is 100% turbulent (Neyrfor, 2004). Consequently, the viscosity is constant (Morrison & Morrison, 2001). This simple fluid model is widely used in similar Turbodrill flow simulations research works (Mokaramian et al., 2013) (V. G. Monteiro, 2017) (Wang, Xia, Wang, Wang, & Zhou, 2016).

In this work a full turbulent numerical model is adopted. ANSYS CFX 2019 R3 CFD package was used for the numerical simulations. A detailed flow field inside the current turbine stage will be investigated. This study aimed to find a relationship between the flow characteristics and their effect on the performance of the turbine.

GOVERNING EQUATIONS

In general, the flow inside turbomachinery is always turbulent. Hence, the flow field (velocity-pressure) is calculated on the basis of Reynolds Averaged Navier-Stokes (RANS) equations. These equations are obtained by considering the time averaged and fluctuation components:

$u_i = U_i + u_i'; \; p = P + p'$

After substituting averaging equations, we obtain the following flow equations (in tensor notation):

$$\frac{\partial \rho}{\partial t} + \frac{\partial (\rho U_j)}{\partial x_j} = 0$$

$$\frac{\partial(\rho U_i)}{\partial t} + \frac{\partial(\rho U_i U_j)}{\partial x_j} = \frac{\partial p}{\partial x_i} + \frac{\partial(\tau_{ij} - \rho \overline{u'_i u'_j})}{\partial x_j} + S_m$$

τ_{ij} is the Reynolds stress tensor defined as follows:

$$\tau_{ij} = \mu(\frac{\partial U_i}{\partial x_j} + \frac{\partial U_j}{\partial x_i}) - \rho \overline{u'_i u'_j}$$

For incompressible Newtonian fluid as the Mud used in the considered turbodrill, the   RANS equations become

$$\rho \frac{\partial U_i}{\partial t} + \rho U_i \frac{\partial U_j}{\partial x_j} + \rho f_i = \frac{\partial p}{\partial x_i} + \frac{\partial}{\partial x_j}(-p\delta_{ij} + 2\mu \overline{S_{ij}} - \rho \overline{u'_i u'_j})$$

f_i is a vector representing body forces, and S_{ij} is the mean rate stain tensor.

$$S_{ij} = \frac{1}{2}(\frac{\partial U_i}{\partial x_j} + \frac{\partial U_j}{\partial x_i})$$

In the current study, k-ε turbulence two-equation model is used to take turbulence effects into consideration (Sagol, Reggio, & Ilinca, 2012).

The standard k-ε model, proposed by Launder and Spalding(Launder, 1972), is based on the assumption that flow is fully turbulent, where the turbulent kinematic energy (*k*) and the energy dissipation rate(*ε) are the main parameters*. The partial differential equations for the standard k-ε model can be written as follows:

$$\frac{\partial}{\partial x_i}(\rho k u_i) = \frac{\partial}{\partial x_j}[(\mu + \frac{\mu_t}{\sigma_k})\frac{\partial k}{\partial x_j}] - \rho \overline{u'_i u'_j}\frac{\partial u_j}{\partial x_i} - \rho\varepsilon + S_k$$

$$\frac{\partial}{\partial x_i}(\rho \varepsilon u_i) = \frac{\partial}{\partial x_j}[(\mu + \frac{\mu_t}{\sigma_\varepsilon})\frac{\partial \varepsilon}{\partial x_j}] - C_{1\varepsilon}\frac{\varepsilon}{k}\rho \overline{u'_i u'_j}\frac{\partial u_j}{\partial x_i} - C_{2\varepsilon}\rho\frac{\varepsilon^2}{k} + S_\varepsilon$$

The eddy viscosity μ_t is calculated according to the following formula:

$$\mu_t = \rho C_\mu \frac{k^2}{\varepsilon}$$

The model coefficients, which are empirically determined, are given as in [14]:

$C_{1\varepsilon} = 1.44$, $C_{2\varepsilon} = 1.92$, $C_\mu = 0.09$, $\sigma_k = 1.0$, $\sigma_\varepsilon = 1.3$

GEOMETRY AND MESH

Turbine stage geometry

The geometry of the stator and the rotor are identical; both have the same diameters of the hub and shroud, which are 108 mm and 134 mm, respectively. The blade height is 14 mm, the pitch of the stator and rotor is 22 mm, and the number of blades is 30 for both (Neyrfor Turbodrill Handbook, 2012). Figure 3 shows the stage configuration.
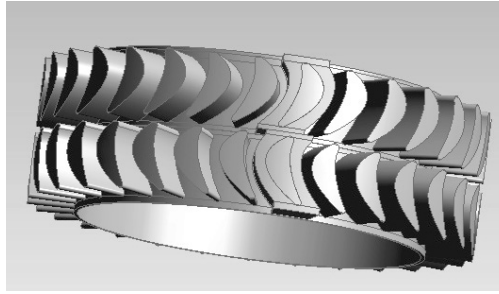
Fig. 3. Turbodrill stage configuration*.*

The main difference between the stator and the rotor is that the latter is unshrouded, and the blade orientation is inversed. The blade geometry specifications were got from inventor patent (Natanael, 2008) to build full blade row by using ANSYS BLADEGEN tool.

Fluid flow inside a Turbodrill

Before proceeding with the 3D simulations and validation, key performance parameters have to be defined on the basis of 1D mean line calculations and velocity triangles (Dixon, 1998). Figure 4 shows the velocity triangles for the studied stage.

The fluid enters the stator with an absolute velocity $\vec{C}_1$ and an inlet angle of α_1; it exits at a velocity $\vec{C}_2$ and an outlet angle α_2. The fluid then enters the rotor at a relative velocity of $\vec{W}_2$, with an angle β_2. At the end of the stage, the flow exits from the whole stage at a velocity $\vec{W}_3$; the exit angle is β_3.
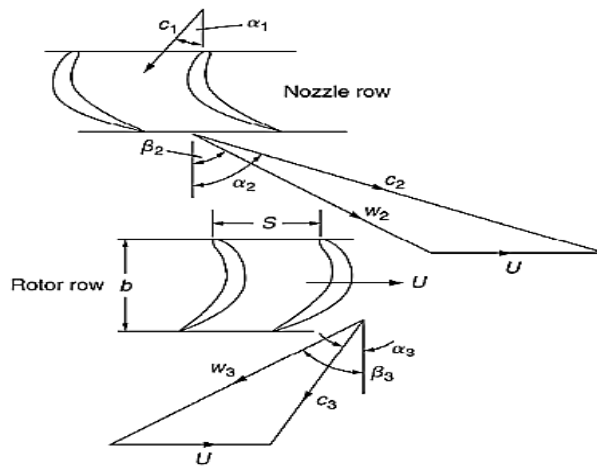

Fig. 4. Axial Turbine stage velocity triangles.

Using the velocity triangles at the design conditions (Dixon, 1998), performance parameters such as power, torque, and the hydraulic efficiency can be evaluated for the turbodrill. On the other hand, these parameters can be measured experimentally on the same realistic geometry of the turbodrill. The numerical results are then to be compared to the measurements.

The hydraulic power generated by each stage of the turbine:

$$P_H = \rho \cdot \dot{m} \cdot U \cdot C_x (tg\beta_2 + tg\beta_3)$$

The output torque of one stage:

$$T = \rho \cdot \dot{m} \cdot r_m \cdot C_x (tg\beta_2 + tg\beta_3)$$

Hydraulic efficiency:

$$\eta_h = \frac{P_H}{\dot{m}\Delta p_{stage}}$$

Mesh sensitivity study

Table 1 shows the mesh cells counts of the whole stage and their influence on power and torque. The tests were conducted under a chosen rotation speed of the rotor Ω=1000 rpm. The global root mean square (RMS) residual was set to 10^{-6}, as the convergence criterion.

Table 1. The hydraulic power and torque at different mesh cells count.

Mesh count	Power (W)	Torque (N.m)
200,000	1465.4	13.994
400,000	1442.5	13.775
600,000	1431.1	13.666
800,000	1429.3	13.649
1,000,000	1424.7	13.605
1,200,000	1421	13.569
1,400,000	1417.5	13.536
1,600,000	1417.6	13.537

From table 1, it is noticed that the values of the power and torque at 1400 K cells are very close to the values at 1600 K cells. Accordingly, the 1400 K cells mesh was selected for the whole simulations to save the computational time and give results that are more accurate.

Boundary Conditions

After building the geometry of the model, it needs to be discretized to a large number of elementary volumes for Finite Volume Method (FVM) and CFD simulation. This process is performed with "TurboGrid" module of ANSYS that creates high quality hexahedral meshes for turbomachinery. The quality of CFD simulation is highly dependent on the density of the mesh.
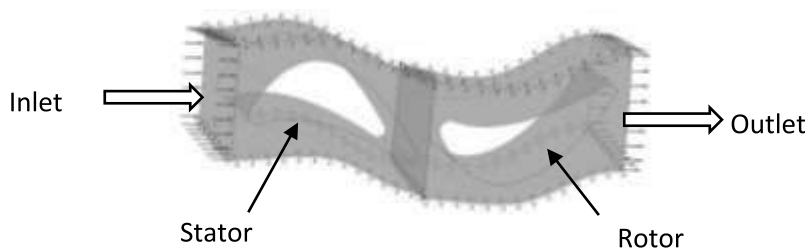

Fig. 5. stator-rotor configuration.

Inlet boundary condition: Fixed pressure=13.78 MPa;

Outlet boundary condition: Mass flow rate = 33.97 kg/s;

No slip: the walls of the blades of stator and the rotor;

Inlet boundary condition: Fixed pressure=13.78 MPa;

Outlet boundary condition: Mass flow rate = 33.97 kg/s;

Wall: stator and the rotor blades: No slip.

For the interaction between the fixed stator and the moving rotor, the stage model (mixing plane) was used as a steady state approach because it is more accurate than the frozen rotor approach because of taking the rotation of the rotor into consideration. Multiple rotation speeds were used for the rotor in the range of Ω=0-2000 rpm. In the current flow simulation, we will use the following physical properties.

Density=1196 kg/m^3,

Viscosity=8.899.10^{-4} kg/m.s,

Thermal conductivity= 0.6069 W/m.K.

CFD SIMULATION RESULTS AND VALIDATION
Validation of the numerical model

Mud flow simulation results are presented in this section. They are also compared to experimental data provided by the manufacturer. Figures 6 and 7 present a comparison between the numerical and experimental values of power and torque for a flow rate of 33.97 kg/s and rotation speed range (0-2000 rpm). The results were achieved after reaching the convergence residuals limit, which was mentioned earlier.
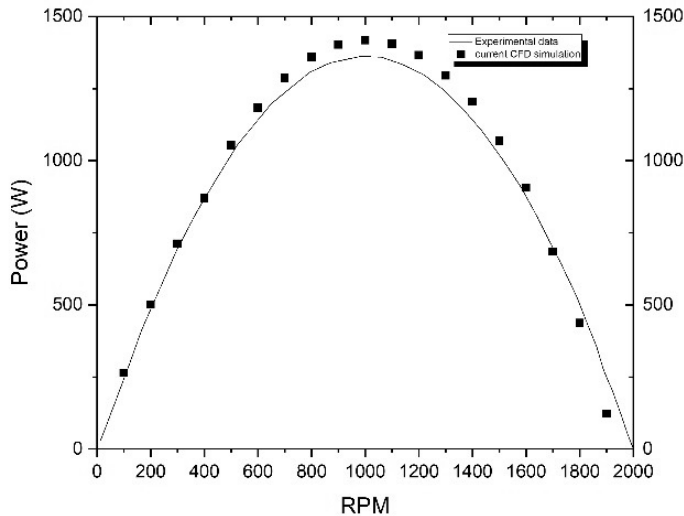

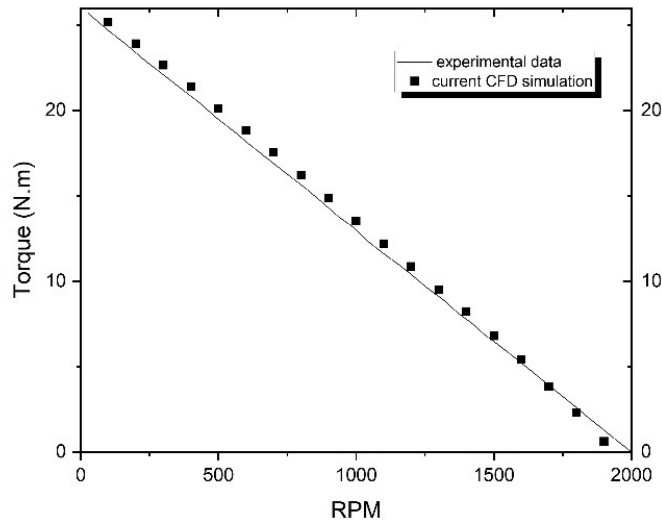**Fig. 6.** Hydraulic power at different rotation speeds.

Fig. 7. Torque at different rotating speeds.

From the previous graphs, it is observed that the CFD results give a very good agreement with the experimental data. Furthermore, this shows that the mixing plane model can be used to estimate the performance curves of this kind of turbines at the used operating conditions with a good accuracy even if it is not a full transient simulation.

The hydraulic power and torque (experimentally and numerically) have the same curve behavior. From the previous plots, it is noticed that optimal power is generated in a small margin around half stall rotation speed. Similarly, at the same conditions, the torque has decreased from a low rotation speed, but it did not affect the performance of the machine. This is because the turbine can give its predicted performance at that torque value at the optimal power value.

Influence of Flow rate density and viscosity of drilling mud on turbodrill performance

It is well known that some operating parameters have more effects than others on turbine performance. These parameters, which we consider as determining parameters, are mass flow rate, Drilling Mud density, and viscosity. In our simulations, we investigate the relationship between the stall torque (maximum torque generated by the turbine at 0 rpm) and the maximum power (generated by the turbine), when varying the determining parameters.

The results are illustrated in tables 2, 3, and 4.

Table 2. Influence of mass flow rate on max power and torque.

Mass flow rate (kg/s)	Max. Power (W)	Stall (max.) Torque (J)
20	273.615	8.83449
24	483.341	12.9073
28	779.53	17.7539
34	1422.35	26.3798
38	2072	32.7729
42	2723	40.7843
46	3606.92	49.1264

This table shows that the variation of mud flow rate produces important qualitative changes in power. More influence on the torque is noted. The obtained results confirm the manufacturer's data (Neyrfor Turbodrill Handbook, 2012).

We conclude that, to ensure a stable operating performance during drilling, a precise monitoring of the mass flow rate is needed. Any slight variation of the mass flow leads to great changes in the performance characteristics of the turbine, which affects negatively the drilling process.

Table 3. Influence of density on max power and torque.

Density (kg/m³)	Max. Power (W)	Stall (max.) Torque (J)
1000	2035	31.6589
1100	1678.87	28.7442
1200	1422.35	26.3798
1300	1200.7	24.296
1400	1035	22.559
1600	796	19.7794
1800	630	17.5905

The density influence on the maximal performances is very pronounced but of lesser degree. On the contrary, optimal power and stall torque decrease when we use more dense mud fluid. This finding must be taken into account when choosing drilling fluids (Neyrfor, 2004).

Table 4. Influence of viscosity on max power and torque.

Viscosity (Pa.s)	Max.Power (W)	Stall (max.) Torque (J)
0.00089	1422.35	26.3798
0.001	1405	26.464
0.0015	1349.07	25.85967
0.002	1305	25.37652
0.003	1245.22	24.5159

The drilling mud viscosity have the least influence on performance. Power and torque decrease slightly when we use Mud that is more viscous. These interesting results proof that the fluid model (viscosity function) has less effect on turbine performance. Nonetheless, it must be taken into account when choosing the best operation conditions for the turbodrill.

Flow fields results

After validation of our CFX simulation, in this section, we will present the results of flow fields. We cannot obtain this kind of information from the manufacturer. It is very difficult to obtain experimentally, especially in field testing conditions.

The following graphs show the flow behavior inside one stage of the current axial turbine at some of the studied rotation speeds. Some key variables like velocity, pressure, and turbulent viscosity are presented in figures 8, 9, and 10.

Three values of impeller rotation speed were considered: low, optimal, and high (400, 1000, and 1600 rpm), respectively. The contours are presented at 50% span of stator and rotor blade regions.
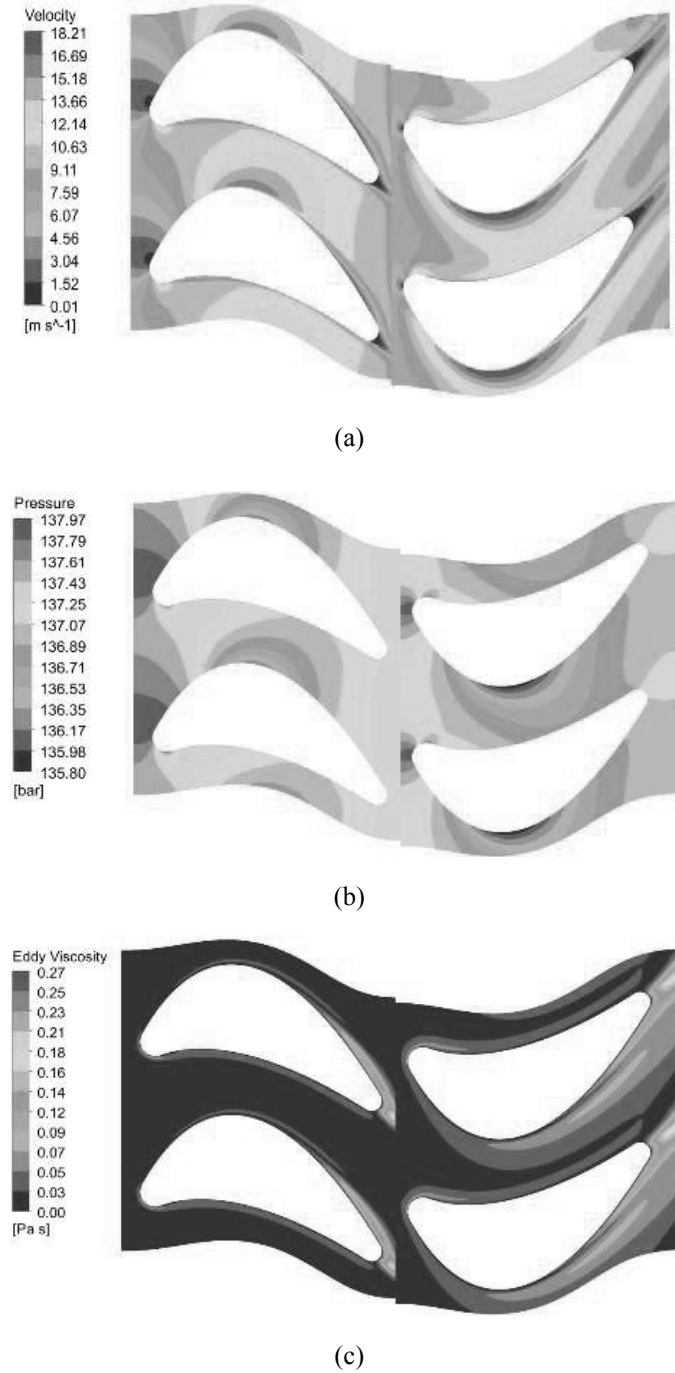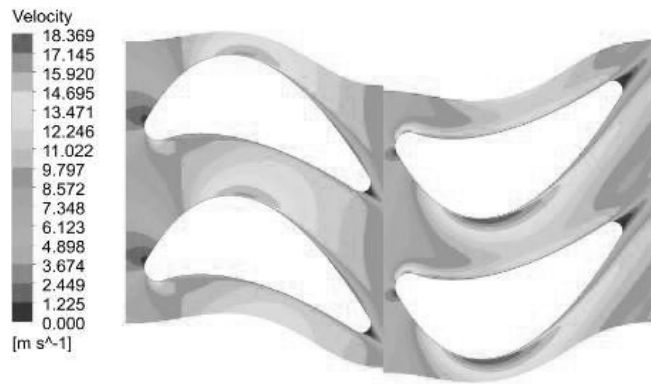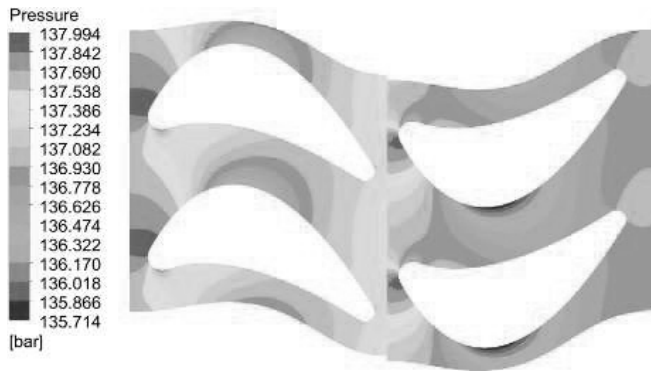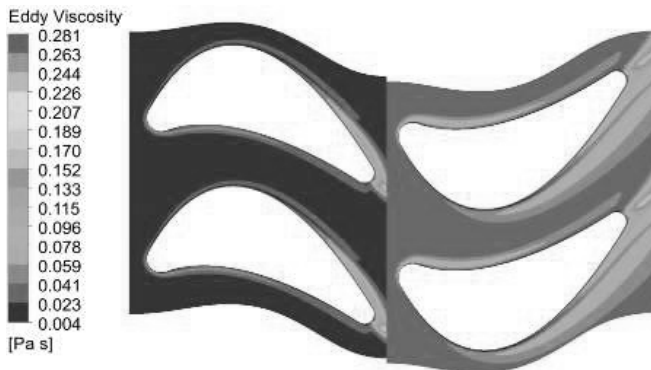

(a)

(b)

(c)

Fig. 8. Flow fields for Ω=400 rpm (a: velocity; b: pressure; c: turbulent viscosity).
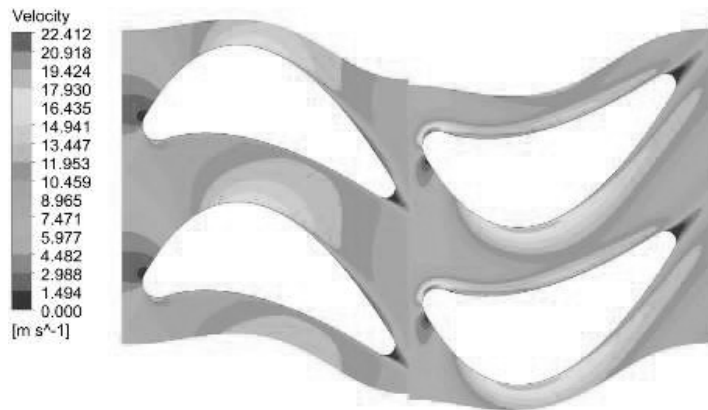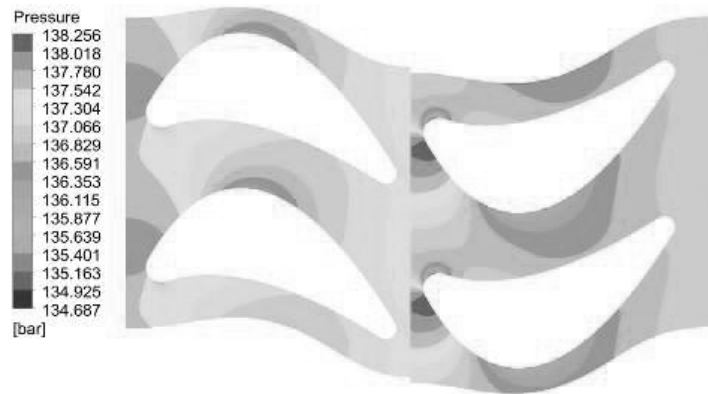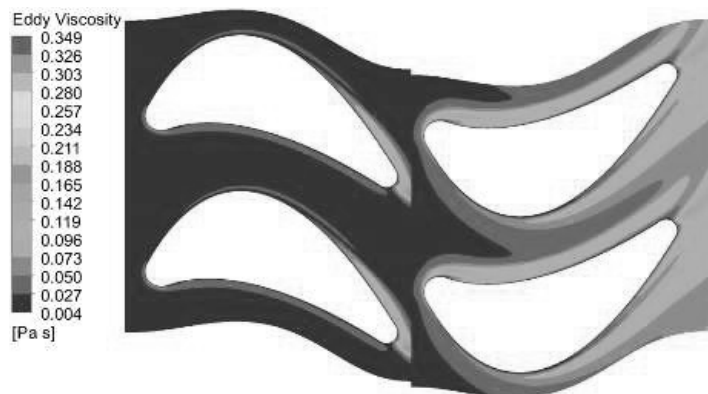
(a)

(b)

(c)

Fig. 9. Flow fields for Ω=1000 rpm (a: velocity; b: pressure; c: turbulent viscosity).

(a)

(b)

(c)

Fig 10. Flow fields for Ω=1600 rpm (a: velocity; b: pressure; c: turbulent viscosity).

It can be observed from these figures that the pressure distribution for the three rotation speed cases is not symmetric around the blades of the rotor and the stator (pressure side and suction side).

This pressure difference is created by the asymmetry of the blade profile geometry, which disturbs the fluid flow

and creates a negative pressure gradient on the suction side and a positive pressure gradient on the pressure side. This creates a lift force mainly for the rotor, leading to the generation of the torque (Murty, 2018).

This pressure distribution also shows the reason of decreasing the torque with increasing the rotation speed (fig. 8b, 9b, and 10b). The pressure difference between blade sides is higher at low rotation speeds. The higher pressure gradient due to the diffusion is taking place for low flow velocity conditions.

In contrast to higher rotation speeds, turbulent effects take over diffusion and bring with them more energy dissipation and turbulent mixing (HITCHENS, 2015). The pressure distribution in this case is more uniform. This leads to a weaker lift force, and the torque is smaller and tends to zero for the maximum rotation speed (stall condition). The velocity field is deeply related to the pressure field. Higher velocity values occur in low pressure regions of the suction side of both stator and rotor.

On the other hand, pressure sides have high pressure and lower velocity. The fluid is firstly accelerated in the stator blades leading edge and when it reaches the throat point, it is decelerated until reaching the leading edge of the rotor blades.

Turbulence is a key factor influencing the turbine performance, and by observing turbulent viscosity, which is an indication of turbulence production, the region around the blade surface is seen especially in the suction side where the velocity values are the highest, and greater turbulence production rates are produced. This trend is seen at the trailing edge of both stator and rotor blade where the boundary layer separation is the main reason for turbulent kinetic energy generation. It is also observed that the turbulent viscosity keeps increasing when the rotation speed is raised from 400 to 1600 rpm, which is predicted since there is more interaction between the blade surfaces and the flowing fluid.

CONCLUSION

In this work, CFD simulations were conducted to simulate the flow of a drilling fluid inside a stage of an axial downhole turbine (Turbodrill). This study has been undertaken to use the CFD tools in order understand the complex behavior of the flow inside this kind of machines. To insure the numerical accuracy, the numerical results of the performance parameters were compared to the measurements provided by the turbine manufacturer.

It was found that the results of the current numerical simulations and the experimental results are in very good agreement. The optimal rotation speed is obtained at 1000 rpm. This is due to establishing a compromise between various physical competing phenomena, namely, diffusion and viscosity forces from one side and inertial and turbulent interactions from the other side.

From this study, it is concluded that the current simulations offer reasonable help in specifying the optimum operating conditions for the considered turbine. In addition, the CFD tool used in this paper can be implemented in future research to investigate all the operating parameters that can influence the function of the turbine and quantify their influences on its performance.

This can be done by running simulations, using the full transient turbulence models like k-ε or shear stress transport and specifying a time step for the simulation to study the interaction between the rotor and stator more precisely.

Nomenclature

U: rotor velocity

Cx: absolute velocity axial component

$\vec{C}$: Absolute velocity

$\vec{W}$: Relative velocity

U_i: Time averaged velocity

u_i: fluctuation velocity

Ω : rotation speed

α_i: absolute angles

β_i: relative angles

T: Torque

P_H: Hydraulic power

ρ : Volumetric mass

r_m: medium radius of the impeller;

ΔP_{stage}: Pressure drop of a stage

ACKNOWLEDGMENT

REFERENCES

Amir Mokaramian, V. R. a. G. C. (2012). *cfd simulations of turbodrill performance with asymmetric stator and rotor blades configuration*. Paper presented at the Ninth International Conference on CFD in the Minerals and Process Industries, CSIRO, Melbourne, Australia.

A. Mokaramian, V. R. a. G. C. (2015). Turbodrill Design and Performance Analysis. *Journal of Applied Fluid Mechanics,* **8**(3), 377-390.

Dixon, S.L. (1998). *Fluid Mechanics,Thermodynamics of Turbomachinery*. Linacre House, Jordan Hill, Oxford OX2 8DP: pergamon Press.

HITCHENS, F.E. (2015). *the encyclopedia of aerodynamics*: Andrews UK Limited.

Launder, B.E. (1972). *Lectures in mathematical models of turbulence, B. E. Launder and D. B. Spalding*. London, New York: Academic Press.

Liguang Wang , Z.L., Yu Wang2, Baolin Liu2 & Qin Zhou (2015). *Flow Field Analysis and Performance Prediction of the Φ127 Turbodrill*. Paper presented at the 5th International Conference on Information Engineering for Mechanics and Materials (ICIMM 2015).

Morrison, F.A. (2001). *Understanding Rheology*: Oxford University Press.

Mokaramian, A., Rasouli, V. & Cavanough, G. (2013). Fluid Flow Investigation through Small Turbodrill for Optimal Performance. *Mechanical Engineering Research,* **3**(1).

Murty, V.D. (2018). *Turbomachinery Concepts, Applications, and Design*: Taylor & Francis Group.

Natanael, M. (2008). USA Patent No. US 7,448,455 B2.

Neyrfor. (2004). *Turbodrill Basics Manual _June 2004*. In S. I. Inc. (Ed.).

Neyrfor Turbodrill Handbook. (2012). In Schlumberger (Ed.).

Robert Radtke, D.G., Dr. Man Mohan Rai. (2011). *high-power turbodrill and drill bit for drilling with coiled tubing* (DE-FC26-06NT15486). Retrieved from Technology International, Inc:

Sagol, E., Reggio, M. & Ilinca, A. (2012). Assessment of Two-Equation Turbulence Models and Validation of the Performance Characteristics of an Experimental Wind Turbine by CFD ISRN Mechanical Engineering. 2012.

V.G. Monteiro, J.T.T., C. Bringhenti, A. Vastenavond & J.H.B. Sampaio Jr. (2017). *performance evaluation of a hydraulic*

turbine used as an turbodrill for oil and gas applications in post-salt environment. Paper presented at the Proceedings of ASME Turbo Expo 2017: Turbomachinery Technical Conference and Exposition, GT2017, Charlotte, NC, USA.

Wang Yu, Y.J. & Li Zhijun. (2014). Design and development of turbodrill blade used in crystallized section. *Scientific World Journal, 2014*, 682963.

Wang, Y., Xia, B., Wang, Z., Wang, L. & Zhou, Q. (2016). Design and Output Performance Model of Turbodrill Blade Used in a Slim Borehole. *Energies,* **9**(12), 1035.

Zhang, X., Yu, S., Gong, Y. & Li, Y. (2016). Optimization design for turbodrill blades based on response surface method. *Advances in Mechanical Engineering,* **8**(2).